Optics Letters

Gigabit Ethernet signal transmission using asynchronous optical code division multiple access

Philip Y. Ma,[1,*] Mable P. Fok,[2] Bhavin J. Shastri,[1] Ben Wu,[1] and Paul R. Prucnal[1]

[1]Lightwave Communications Laboratory, Department of Electrical Engineering, Princeton University, Princeton, New Jersey 08544, USA
[2]Lightwave and Microwave Photonic Laboratory, College of Engineering, University of Georgia, Athens, Georgia 30602, USA
*Corresponding author: yechim@princeton.edu

Received 23 September 2015; revised 19 November 2015; accepted 19 November 2015; posted 20 November 2015 (Doc. ID 250006); published 15 December 2015

We propose and experimentally demonstrate a novel architecture for interfacing and transmitting a Gigabit Ethernet (GbE) signal using asynchronous incoherent optical code division multiple access (OCDMA). This is the first such asynchronous incoherent OCDMA system carrying GbE data being demonstrated to be working among multi-users where each user is operating with an independent clock/data rate and is granted random access to the network. Three major components, the GbE interface, the OCDMA transmitter, and the OCDMA receiver are discussed in detail. The performance of the system is studied and characterized through measuring eye diagrams, bit-error rate and packet loss rate in real-time file transfer. Our Letter also addresses the near-far problem and realizes asynchronous transmission and detection of signal.

OCIS codes: (060.2330) Fiber optics communications; (060.2360) Fiber optics links and subsystems.

http://dx.doi.org/10.1364/OL.40.005854

Incoherent optical code division multiple access (OCDMA) has been studied intensively due to its unique networking advantages, including asynchronous access, soft blocking, switchless packet transmission, increased spectral efficiency (with M-ary modulation), and flexible provisioning of differentiated quality of service (QoS) [1–5]. A huge number of users can be supported using a minimal number of wavelengths through the soft blocking characteristic by having each of the OCDMA codes share the same wavelengths with different code sequences. Moreover, by assigning even fixed code with different code lengths and weights, incoherent OCDMA networks can carry heterogeneous traffic with different data rate and errors for each subscriber, enabling much more flexible allocation of the network bandwidth than other conventional multiplexing techniques such as time division multiplexing (TDM) or wavelength division multiplexing (WDM) [6]. OCDMA also provides a protocol-independent physical transmission layer; thus, it is suitable to be used for various types of networks. The unique advantages and characteristics of both coherent [7–9] and incoherent [10–12] OCDMA have been studied and investigated intensively in recent years.

Ethernet technology has been the most commonly used computer networking technology in the local area networks (LANs). With the fiber-optic network as the backbone, it has been the most widely spread wired LAN technology. To utilize the capacity of optical LANs, the use of OCDMA becomes particularly attractive. The transmission of fast Ethernet [13] and Gigabit Ethernet [14] over OCDMA have been previously demonstrated using coherent and incoherent OCDMA, respectively.

In this Letter, we propose and experimentally demonstrate an architecture for interfacing and transmitting a Gigabit Ethernet (GbE) signal over asynchronous incoherent OCDMA. Unlike previous architecture, our approach does not require the distribution of a central clock to each transmitter and receiver, thus supporting independent clock rates for each user and truly asynchronous operation of the system without waiting for the designated transmission time slot. The laser source is generated from distributed feedback laser diodes (DFB-LDs), while the data rates of each OCDMA signal are asynchronous and governed by each of the Ethernet signals. The receiver exploits a four-wave mixing (FWM) wavelength-aware receiver for multi-access interference (MAI) removal, together with a semiconductor optical amplifier (SOA) for amplitude noise suppression [15]. The signal is converted to an electrical format using a band-limited low-speed photodetector such that non-return-to-zero (NRZ) signals result for interfacing with a standard clock and data recovery (CDR) system for asynchronous detection. With the use of media converter, the signals are converted to Ethernet data easily, and real-time file transfer is achieved. The measurements of eye diagrams, bit-error rate, and packet loss rate are thereby performed and discussed.

Figure 1 shows the asynchronous incoherent OCDMA architecture transmitting Ethernet signals among four users: 1, 2, 3, 4. The whole system consists of three major components: the GbE interface, the OCDMA transmitter, and the OCDMA receiver.

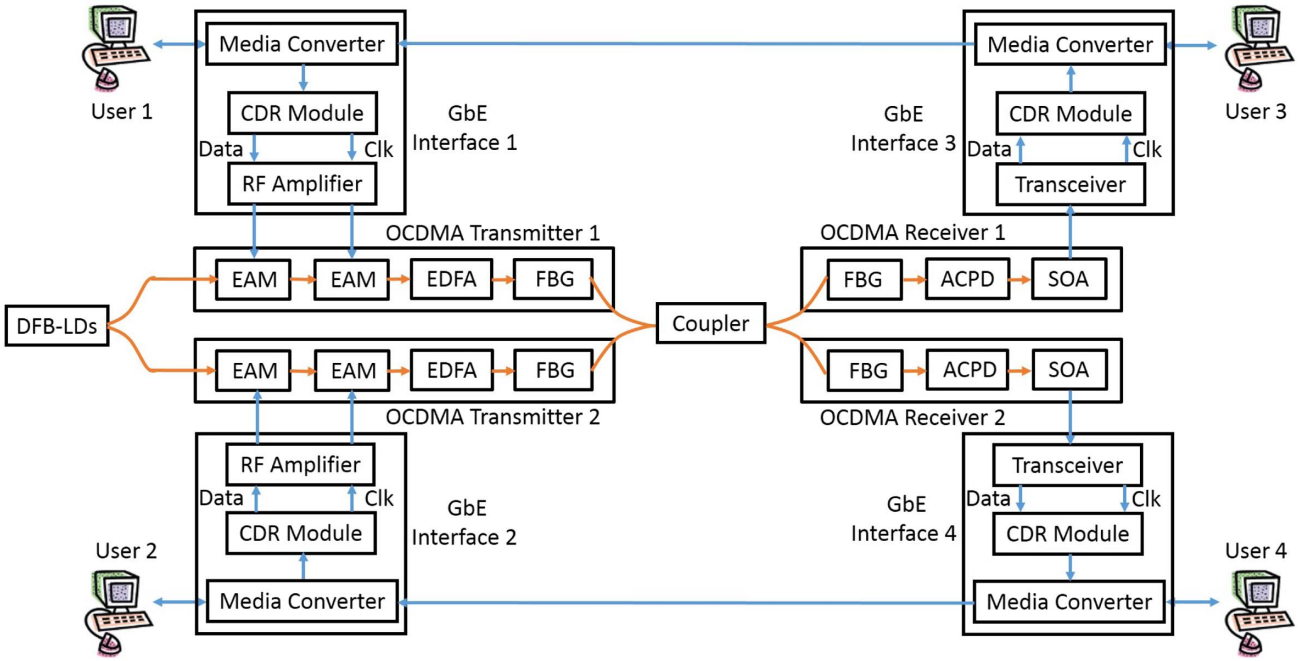

Fig. 1. Asynchronous incoherent OCDMA architecture interfacing Gigabit Ethernet. (CDR, clock and data recovery; DFB-LDs, distributed feedback laser diodes; EAM, electro-absorption modulator; EDFA, erbium-doped fiber amplifier; FBG, fiber Bragg grating; ACPD, auto-correlation peak discriminator; SOA, semiconductor optical amplifier.)

The GbE Interface bridges between the devices operating on optical signals and those operating on electronic signals. Ethernet ports of all the four computers are connected to a media converter through a bidirectional LAN cable for the conversion between Ethernet data and NRZ signals. On the OCDMA transmitter side, the NRZ signals are launched to the CDR module, where a clock signal can be extracted from the NRZ signal and separated from the data. The extracted clock and data signals are then amplified by a radio-frequency (RF) amplifier before entering the OCDMA transmitter. The GbE interface on the OCDMA receiver side works in a similar way, except for the replacement of the RF amplifier with a transceiver. The transceiver takes the advantage of a low-speed (1.25 Gb/s) photodetector to band-limit the return-to-zero (RZ) OCDMA receiver output and converts it to an NRZ electrical signal that perfectly interfaces with the CDR module. The recovered clock and data are then launched to the media converter for the conversion to Ethernet data. Note here that we only connect the media converters of User 3 and 4 back to those of Users 1 and 2, respectively, for completing the communication paths between two pairs of OCDMA transmitters and receivers but, in general, these four media converters can be interconnected.

The incoming clock and data signals are used to generate OCDMA signals through pulse carving and data modulation at two electro-absorption modulators (EAMs). The optical source being modulated comes from a DFB-LDs module, where the following three wavelengths are used: 1550.17, 1551.90, and 1553.30 nm. The optical signals carrying the clock and data information are optically amplified before being encoded by fiber Bragg grating (FBG) arrays using wavelength-hopping time-spreading (WHTS) codes with 17 time chips within one bit. The weight sequences for Encoders 1 and 2 are (0, 3, 6) and (0, 7, 14), respectively, where the numbers correspond to the chip positions relative to the first wavelength. After encoding for both Users 1 and 2, the OCDMA signals are then combined by a 50:50 coupler and transmitted to the OCDMA receiver side. It is worth mentioning here that transmitters (as well as receivers, as discussed below) all operate on their own clock rates determined by the Ethernet data they are transmitting, rather than a centralized one, which demonstrates true asynchronization.

In order for Users 3 and 4 to receive the signals, the OCDMA signals have to be first decoded by corresponding FBG arrays, where they align all the spectral components of the targeted code in time to form an autocorrelation peak while spreading the spectral components of the interfering users over time as MAI. MAI needs to be removed by an auto-correlation peak discriminator (ACPD) to avoid detection failure and, in our design, a FWM wavelength-aware receiver is employed. An FWM wavelength-aware receiver is made up of a 40 m highly Ge-doped nonlinear fiber (HDF) for FWM and a 4 nm optical notch filter for blocking the MAI after FWM. The HDF has 75 mol.% GeO_2, resulting in a large nonlinear coefficient of 35 $W^{-1}\,km^{-1}$ [16]. In addition to MAI, the amplitude noise at the HDF and photodetector introduced by the overlapping of the autocorrelation peak and MAI is another factor that degrades signal detectability [17,18]. Therefore, an SOA is used to reduce the amplitude noise within the FWM wavelength-aware receiver output.

The users can operate in a synchronous way, with all users at a centralized data rate of 1.25 Gb/s, or in an asynchronous way where each user has its own individual data rate which is not synchronized among each other. Suppose User 1 is the main user while User 2 acts as the interfering user at the receiver for User 1; then, in asynchronous operation, User 1 operates at

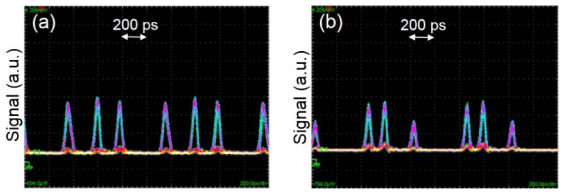

Fig. 2. Encoded OCDMA signal output of the OCDMA transmitters of two users: (a) User 1 and (b) User 2.

1.249974 Gb/s while User 2 operates at 1.249972 Gb/s. Each user has its unique code sequence after encoding as shown in Fig. 2 with 40 ps full-width at half-maximum pulses.

After decoding, the power of the MAI (P_M) could be smaller or larger than that of the autocorrelation peak (P_A) due to the near-far effect. Figure 3 considers the successful extraction of autocorrelation peak in terms of different P_M/P_A ratios. Figure 3(a) shows the decoded signal inside OCDMA receiver at a 0 dB P_M/P_A ratio, with both autocorrelation peaks and MAI observed. Figure 3(c) shows the decoded signal with P_M/P_A ratio of 2 dB, where the amplitudes of the autocorrelation peaks and MAI peaks become indistinguishable. As we increase the P_M/P_A ratio to 6 dB, the intensity of MAI is even larger than that of autocorrelation peaks, as shown in Fig. 3(e). The importance of FWM wavelength-aware receiver lies in the fact that it is capable of removing the resulted MAI completely, no matter how strong it is, as evidenced in Figs. 3(b), 3(d), and 3(f).

In a real OCDMA system, the overlapping of MAI and the autocorrelation peak cannot be avoided in many cases, especially with asynchronous operation. The overlapping leads to severe amplitude noise resulting from FWM and beating in nonlinear fibers and photodetectors. We utilize an SOA in our OCDMA receiver to reduce the amplitude noise before the 1.25 Gb/s photodetector. If we make a comparison between the eye diagrams shown in Figs. 4(a) and 4(b), noise reduction definitely plays an indispensable role in helping to open the eye in its middle region.

For the GbE interface on the OCDMA receiver side, the MAI removal exhibits even more significance as the performance of transceiver and CDR module can be severely degraded by MAI. Figure 5 shows the eye diagrams observed at the transceiver

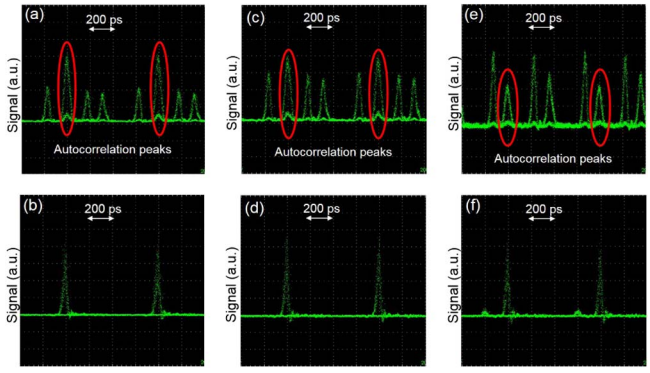

Fig. 3. Decoded OCDMA signal at the OCDMA receiver of User 1. (a) Without MAI removal and $P_M/P_A = 0$ dB, (b) with MAI removal and $P_M/P_A = 0$ dB, (c) without MAI removal and $P_M/P_A = 2$ dB, (d) with MAI removal and $P_M/P_A = 2$ dB, (e) without MAI removal and $P_M/P_A = 6$ dB, and (f) with MAI removal and $P_M/P_A = 6$ dB.

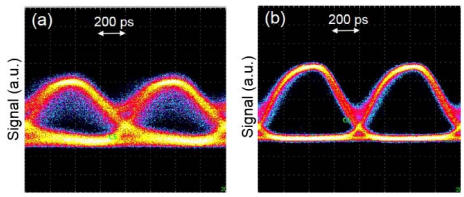

Fig. 4. Eye diagrams of (a) decoded OCDMA signal after only MAI removal and (b) decoded OCDMA signal after both MAI removal and amplitude noise suppression.

and CDR module for different P_M/P_A ratios. When the MAI power is comparable to that of autocorrelation peaks [Fig. 5(a)], neither transceiver nor CDR module performs well in signal detection. As we decrease the P_M/P_A ratio to −2 dB [Fig. 5(b)], the eye diagrams at both transceiver and CDR module start to take shape, while their MAI tolerance are not exactly consistent. It is evident that while the recovered clock and data signal may show a clear eye, the OCDMA receiver output signal may still not be correct at the transceiver, and the reason could be attributed to the fact that NRZ-like optical CDMA signal interfaces better with the CDR module than the RZ-like OCDMA signal with transceiver. Only when we are able to reduce the P_M/P_A ratio to be as low as −9 dB [Fig. 5(c)] can the eye diagrams at both the transceiver and CDR module behave as they do without MAI [Fig. 5(d)].

The bit-error rate (BER) measurements of the OCDMA signal at both the transceiver and CDR module are shown in Fig. 6. Once again, we have to emphasize the importance of MAI removal, and we consider minus PM/PA ratio to show the importance of MAI removal; even a small amount of MAI residual could result in diversified BER curves compared to a no-MAI case. At the absence of FWM wavelength-aware receiver, the CDR module presents a better BER over the transceiver since it has a greater tolerance of MAI as shown above. The BER improves quickly with a decrease in MAI power and approaches the no-MAI curve when the P_M/P_A ratio could be restricted to be less than −9 dB for transceiver and less than −6 dB for CDR module. A typical 10^{-9} BER could be obtained at −24 dBm receiver power under perfect MAI removal.

We conduct real-time file transfer for our OCDMA system as well. Among all four users, we ask Users 1 and 2 to send files

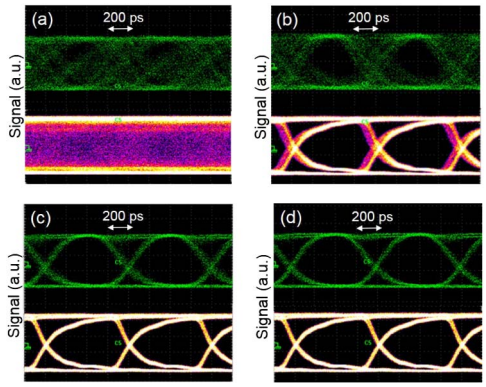

Fig. 5. Eye diagrams observed at transceiver (up) and CDR module (down) of User 3. (a) Without MAI removal and $P_M/P_A = 0$ dB, (b) without MAI removal and $P_M/P_A = -2$ dB, (c) without MAI removal and $P_M/P_A = -9$ dB, and (d) with MAI removal.

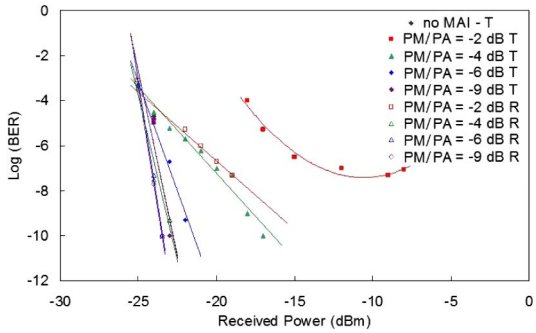

Fig. 6. BER measured at transceiver and CDR module of User 3. T, transceiver; R, clock and data recovery module.

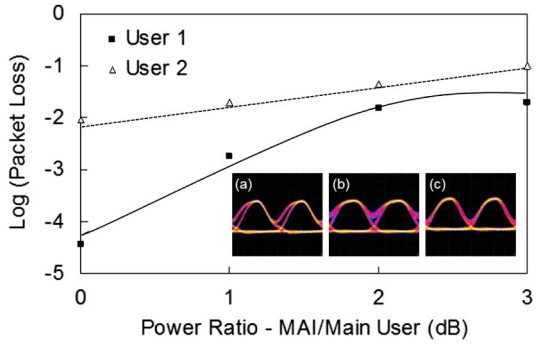

Fig. 7. Packet loss rate using TCP protocol measured at different MAI/Main User ratios. Insets: eye diagrams of transceiver against input optical power of (a) −14 dBm, (b) −18 dBm, and (c) −22 dBm.

to Users 3 and 4 using TCP protocol. It normally takes 1 min to complete the transfer of a 200 MB file. Meanwhile, we measure the packet loss rate during the file transfer, as shown in Fig. 7. The packet loss rate that is acceptable depends on the type of data being sent but, normally, less than 1% packet loss is "good," and 1–3% is "acceptable." Apparently, the packet loss rate of the system is sensitive to the input power of each user. With a power ratio of MAI/Main User = 0 dB (input optical power to transceiver is −23 dBm for User 1 and −20 dBm for User 2, input optical power is measured when serving as the Main User), User 1 has a packet loss rate of 0.003%, while User 2 has a packet loss rate of 1% which requires more optimization. The packet loss rate difference could be attributed to the fact that the performance of transceiver can also be affected by the OCDMA receiver output power (insets of Fig. 7) and a finer tuning of the OCDMA Receiver 2 is needed. Considering the near-far effect with a power ratio of MAI/Main User = 3 dB (input optical power to transceiver is −18 dBm for User 1, −15 dBm for User 2), both users present higher packet loss rates with User 1 to be 1.9% and User 2 to be 10%. Further improvements could be made to improve the amplitude noise suppression on beating within nonlinear fibers.

We have experimentally demonstrated a novel asynchronous OCDMA scheme that allows GbE signal transmission among multiple users. Each user is able to perform data transmission with individual clock rate and asynchronous data rate. Detailed structure designs are presented for a GbE interface, OCDMA transmitter, and receiver. MAI from the OCDMA system is removed completely based on an FWM wavelength-aware receiver, and the near-far issue is addressed. The complete removal of MAI allows the use of a low-speed photodetector with the same data rate as the OCDMA signal without any interference from MAI. It also allows the OCDMA signal to be interfaced with a CDR system to realize asynchronous detection by converting the RZ OCDMA signal into an NRZ electrical signal that inherently satisfies the input requirements of digital communication systems. SOA is employed to reduce the amplitude noise introduced by the overlapping of MAI with the autocorrelation peak as well. System performance is evaluated under harsh conditions by measuring the BER and packet loss rate in real-time file transfer.

Funding. National Science Foundation (NSF) (ECCS 1247298).

Acknowledgment. The authors would like to thank Dr. Yanhua Deng for assistance in building the system.

REFERENCES

1. P. R. Prucnal, *Optical Science and Engineering* (CRC Press, 2005).
2. J. A. Salehi, J. Opt. Netw. **6**, 1138 (2007).
3. C.-S. Brès, Y.-K. Huang, I. Glesk, and P. R. Prucnal, J. Opt. Netw. **6**, 599 (2007).
4. C.-S. Brès, I. Glesk, R. J. Runser, T. Banwell, P. R. Prucnal, and W. C. Kwong, *Proceedings of Lasers and Electro-Optics Society Annual Meeting-LEOS*, Sydney, Australia (IEEE, 2005), pp. 967–968.
5. V. Baby, C.-S. Brès, L. Xu, I. Glesk, and P. R. Prucnal, Electron. Lett. **40**, 755 (2004).
6. P. R. Prucnal, M. P. Fok, K. Kravtsov, Z. Wang, and Y. Deng, *LEOS Summer Topical Meeting*, Newport Beach, California (IEEE, 2009), pp. 9–10.
7. J. Liu, Y. Lu, C. Guo, X. Hong, L. Xu, and S. He, IEEE Photonics Technol. Lett. **22**, 583 (2010).
8. W. Amaya, D. Pastor, R. Bños, and V. Garcia-Munoz, Opt. Express **19**, 24627 (2011).
9. Y. Yang, M. Foster, J. B. Khurgin, and A. B. Cooper, Opt. Express **20**, 17600 (2012).
10. J. Penon, W. Mathlouthi, S. LaRochelle, and L. A. Rusch, J. Lightwave Technol. **27**, 108 (2009).
11. Z. Wang, J. Chang, and P. R. Prucnal, J. Lightwave Technol. **28**, 1761 (2010).
12. A. Lalmahomed, M. M. Karbassian, and H. Ghafouri-Shiraz, J. Lightwave Technol. **28**, 39 (2010).
13. J. Hu, W. Cong, V. Hernandez, B. Kolner, J. Heritage, and S. Yoo, *Optical Fiber Communication and the National Fiber Optic Engineers Conference-OFC/NFOEC*, (IEEE, 2007), pp. 1–3.
14. Y. Deng, M. P. Fok, and P. R. Prucnal, *IEEE Photonics Society Summer Topical Meeting Series*, Montreal, Quebec City, July 18, 2011.
15. M. P. Fok, Y. Deng, and P. R. Prucnal, Opt. Lett. **35**, 1097 (2010).
16. E. M. Dianov and V. M. Mashinsky, J. Lightwave Technol. **23**, 3500 (2005).
17. J. A. Armstrong, J. Opt. Soc. Am. **56**, 1024 (1966).
18. X. Wang and K. I. Kitayama, J. Lightwave Technol. **22**, 2226 (2004).